Pharmacogn J. 2022; 14(6) Suppl: 1005-1021
A Multifaceted Journal in the field of Natural Products and Pharmacognosy
www.phcogj.com

Research Article

DFT and Pharmacokinetic Study of Some Heterocyclic Aspirin Derivatives as The Cyclooxygenase Inhibitors: An *In-Silico* Approach

Emranul Kabir[1, 2,*], M. R. O. Khan Noyon[1], Md. Amjad Hossain[1], Pranta Acharjee[1]

ABSTRACT

Ibuprofen and aspirin are frequently used to relieve inflammation, pain, and fever. These are the two most significant non-steroidal and anti-inflammatory drugs (NSAIDs). They prevent the development of prostaglandin by blocking the function of cyclooxygenase (COX). The biological and physiochemical aspects of some hetero-cyclic aspirin derivatives have been investigated, and the compounds have been assessed by ibuprofen as well as quantum mechanical computations. Density functional theory (DFT) with the B3LYP/6-31G+ basis function has been used to elucidate the thermo-chemical, molecular orbital, and optimum geometrical aspects in the gas phase. Using molecular docking and non-bonding interactions, the binding affinities and behaviors of some heterocyclic aspirin analogs have been studied on human cyclooxygenase (COX-1 as well as COX-2) proteins (6Y3C and 5F19). The chemical stability of all structures is supported by geometry and thermo-chemical findings. In contrast to aspirin and ibuprofen, almost all tested analogs exhibited a substantial binding score to the receptor protein (5F19). The ADMET prediction revealed the enhanced pharmacokinetic properties of some derivatives with less acute oral toxicity. Overall, eight heterocyclic aspirin analogues 2-9 were shown to be more effective in inhibiting Cyclooxygenase-2 (5F19) than Cyclooxygenase-1 (6Y3C), indicating that they may be effective as COX-2-related inflammation therapeutic candidates.
Key words: Aspirin, Heterocyclic compound, DFT, Molecular docking, ADMET.

Emranul Kabir[1, 2,*], M. R. O. Khan Noyon[1], Md. Amjad Hossain[1], Pranta Acharjee[1]

[1]*Faculty of Science, Department of Chemistry, University of Chittagong, Chittagong, 4331, BANGLADESH.*

[2]*Department of Electrical and Electronic Engineering, International Islamic University Chittagong, Chittagong, 4318, BANGLADESH.*

Correspondence

Emranul Kabir

Faculty of Science, Department of Chemistry, University of Chittagong, Department of Electrical and Electronic Engineering, International Islamic University Chittagong, Chittagong, 4318, BANGLADESH.

E-mail: ekabir05@gmail.com

History

- Submission Date: 26-10-2022;
- Review completed: 10-12-2022;
- Accepted Date: 15-12-2022.

DOI : 10.5530/pj.2022.14.204

Article Available online

http://www.phcogj.com/v14/i6

INTRODUCTION

Aspirin has been employed as a medication to treat fever and inflammation for more than a century. It has been previously described how aspirin works biologically.[1-3] On the basis of antithrombotic activity in platelets and the suppression of cyclooxygenase by aspirin, which is essential for blood clotting, its usage has recently been expanded to include the treatment and prevention of cardiovascular disease.[4] When used at modest doses to treat angiotensin-sensitive primigravida with preeclampsia, pregnancy-induced hypertension, and other forms of coronary artery disease, aspirin's anti-platelet activity has generally had positive outcomes.[5] However, aspirin's adverse effects, like gastrointestinal harm and vulnerable oxidation, are quite serious.[6] According to clinical research, gastrointestinal damage from COX-2 selective medicines with anticancer activity is low. Therefore, it might be preferable to create new aspirin derivatives that inhibit COX-2 rather than COX-1 more effectively.[7] The search for new aspirin derivatives has recently gained a lot of scholarly attention as researchers seek to alter and modify aspirin's structural composes. In an attempt to lessen the gastrointestinal adverse effects of aspirin, acetylsalicylic acid copper, aspirin zinc, and vanadium-aspirin have been developed; however the results haven't been promising.[7-9] In addition to reducing intestinal inflammation and tumor growth *in vivo*, resveratrol and also its aspirin analogues can suppress nuclear factor kappa B (NF-B) activation, cytokine production, and the rate at which cancer cells proliferate. DNA methyltransferase (DNMT) activity, cyclooxygenase (COX) efficacy, and cytochrome P450 activity can all be inhibited by resveratrol-aspirin derivatives.[10] Moreover, the adverse effects of aspirin on the gastrointestinal tract can be minimized by incorporating a nitric oxide (NO)-releasing moiety into the drug. Once more, the combination of NO generation and COX restriction in furoxan-aspirin may represent a novel strategy to reduce platelet aggregation.[11] So, creating novel aspirin derivatives with improved cyclooxygenase (COX) and anti-cancer activity compared to aspirin with fewer gastrointestinal side effects would be a sensible option. The COX activity of aspirin compounds and heterocyclic derivatives has been demonstrated in recent years.[12] A suitable strategy to maintain aspirin's COX-inhibiting capabilities while lowering its stomach toxicity is the mixing of aspirin and heterocyclic analogues. In this research, we report the results of thermodynamic, molecular orbital, electrostatic potential, geometric, FT-IR, UV-Vis, molecular docking, non-bonding interactions, and ADMET prediction assessments of a few heterocyclic aspirin analogs. The majority of the derivatives displayed enhanced interactions, reactivity, thermal stability, and binding affinities. Hydrogen bonds play a vital role in biological processes because they affect the system's thermodynamic and structural stability.[12-15]

METHODS AND MATERIALS

Structures of aspirin (1), heterocyclic aspirin derivatives (2–9) and ibuprofen (10)

In our research, aspirin (1), its 2-acetoxyphenyl derivatives (2-9) and ibuprofen (10) are selected

Cite this article: Kabir E, Noyon MROK, Hossain MA, Acharjee P. DFT and Pharmacokinetic Study of Some Heterocyclic Aspirin Derivatives as the Cyclooxygenase Inhibitors: An *In-Silico* Approach. Pharmacogn J. 2022;14(6)Suppl: 1005-1021.

for DFT, pharmacokinetic and COX potentiality study in Figure 1. A research team Asma *et al.*[16] has already synthesized these compounds. Structurally, all of the heterocyclic aspirin derivatives (2-9) contain different heterocyclic moieties which are connected with phenyl acetate *via* alkane functional group (C-C single bond) at C-1 position of aspirin (1) (Figure 1).

Geometry optimization

The basic geometry of aspirin (1) (CID 2244) and Ibuprofen (10) (CID 3672) were collected from the online structural database PubChem.[17] By using aspirin structure, the required molecules 2-9 were generated in the Gauss View (5.0) software.[18] By employing the Amber force field and the Berendsen theory in Gabedit software (version 2.5.0), a molecular dynamics simulation was performed to find the lowest energy conformer.[19] The Gaussian 09W Revision D.01 program was used to perform geometry optimization.[20] Incorporating density functional theory (DFT)[21-23] and the B3LYP 6-31G+[24,25] level of theory, all geometries were optimized and their thermodynamics, molecular orbital, electrostatic potential and vibrational frequencies were clarified by using previously reported approaches.[26] Time-dependent density functional theory (TD-DFT) was used to calculate electronic absorption and transition.[27]

Protein preparation, molecular docking and interaction calculation

Molecular docking technology is used to predict the interactions and changes in binding conformation between substances, ligands, and protein binding sites. Over the course of the last three decades, a number of molecular docking programs have been developed. Many of the popular programs are still in use today, enabling scientists to learn how various substances interact with one another.[28] Docking was accomplished on structures 1-10 that were optimized (described in section 2.1). Two significant proteases, cyclooxygenase-1 (6Y3C) and cyclooxygenase-2 (5F19), and their three-dimensional crystal structures were obtained in pdb format from RCSB proteins data library.[26,29] PyMOL (Version 1.7.4) was used to remove water and unnecessary hetero-atoms from 6Y3C and 5F19, and the files were also saved in pdb format.[30] The energy of each ligand was minimized with the help of the Swiss PDB software (version 4.1.0).[31] Using PyRx (Version 0.8) autodock vina, we performed molecular docking with all the chemicals and proteins in usable formats.[32] Auto docking was carried out by loading the ligands and proteins after the box size was set to the maximum dimension level (according to software command). When docked complexes were queried in Discovery Studio 4.1(client), the necessary non-bond interactions were calculated.33

ADMET prediction

The pharmacokinetic parameters of organic compounds i.e."absorption, distribution, metabolism, excretion, and toxicity (ADMET)", can be predicted using a variety of software applications. Here, the ADMET of heterocyclic aspirin derivatives 2-9 were predicted utilizing *admetSAR* protocol (http://lmmd.ecust.edu.cn/admetsar1/home/).[34] ADMET of the investigated compounds 2-9 were presented in Table 6. The results were predicted in each case using structural data files and the simplified molecular input line entry system (SMILES).

Quantitative structure-activity relationship (QSAR)

About 633 descriptors are included in the ChemoPy (python program) descriptors from the ChemDes (http://www.scbdd.com/chemdes/) (chemical descriptors) repository.[35] Most of the eight descriptors that were described by a cross-validation technique and a genetic search algorithm approach were connected with biological processes and molecular docking studies. To forecast the correlation between quantitative structure and activity (QSAR), a model was created using multi-linear regression (MLR) equations.[36]

Here, pIC_{50} (Activity) = −2.768483965 + 0.133928895 × (Chiv5) + 1.59986423 × (bcutm1) + (−0.02309681) × (MRVSA9) + (−0.002946101) × (MRVSA6) + (0.00671218) × (PEOEVSA5) + (−0.1596341 5) × (GATSv4) + (0.207949857) × (J) + (0.082568569) × (Diameter).

RESULTS AND DISCUSSION

Thermo-chemical analysis

The most crucial thermo-chemical concepts for evaluating association and reaction tendencies as well as the chemical stability of the reaction products are free energy, enthalpy, and dipole moment. Free energy and enthalpy play an essential role in a chemical reaction's energy absorption or release as well as the chemical stability of the molecule. The value of free energy elucidates the degree of spontaneity of the adsorption process[37,38] and the negative sign indicates the spontaneity condition of a reaction.[39] No external energy will be required for bonding because all of the compounds' free energy and enthalpy values are negative (Table 1) in this situation. Due to the presence of high electronegative atoms Oxygen (O) and Sulphur (S), compounds 7 and

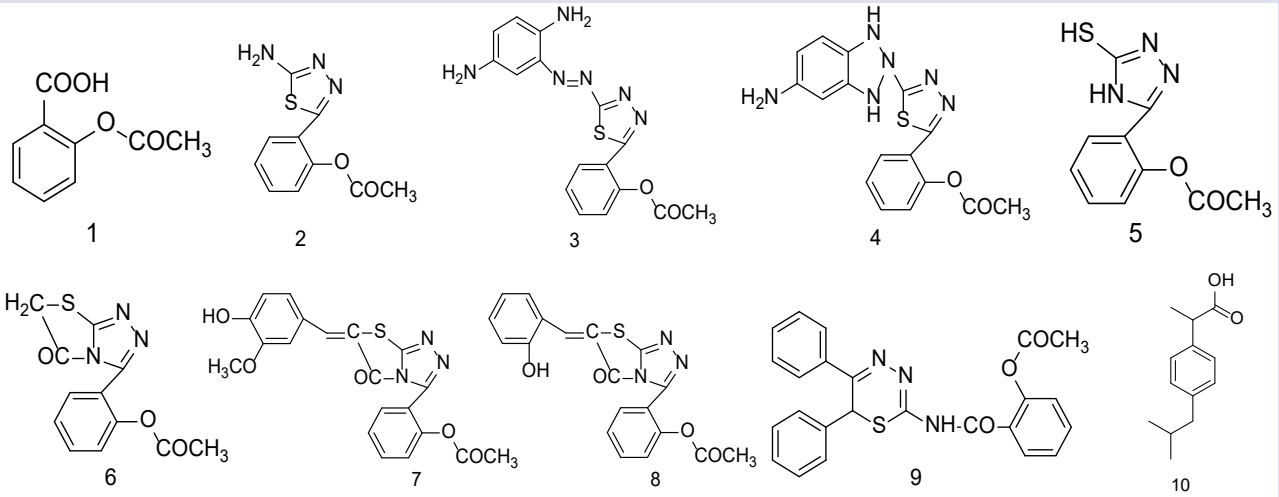

Figure 1: Structures of aspirin (1), heterocyclic aspirin derivatives (2-9) and ibuprofen (10).

Table 1: Molecular formula (MF), molecular weight (MW), energies (Hartree) and dipole moment (Debye) of aspirin (1), Heterocyclic aspirin derivatives (2–9) and ibuprofen (10).

Compound	MF	MW	Internal energy	Enthalpy	Free energy	Dipole moment
1	$C_9H_8O_4$	180.16	-648.353	-648.352	-648.404	5.301
2	$C_{10}H_9N_3O_2S$	235.26	-1098.944	-1098.943	-1099.003	4.400
3	$C_{16}H_{16}N_6O_2S$	356.40	-1494.559	-1494.558	-1494.637	6.221
4	$C_{16}H_{16}N_6O_2S$	356.40	-1494.547	-1494.546	-1494.619	4.352
5	$C_{10}H_9N_3O_2S$	235.26	-1098.943	-1098.942	-1099.001	5.070
6	$C_{12}H_{10}N_3O_3S$	276.29	-1250.300	-1250.299	-1250.360	5.908
7	$C_{20}H_{15}N_3O_5S$	409.42	-1708.960	-1708.959	-1709.044	7.066
8	$C_{19}H_{14}N_3O_4S$	380.40	-1594.495	-1594.494	-1594.568	5.045
9	$C_{24}H_{19}N_3O_3S$	429.49	-1713.325	-1713.324	-1713.412	5.395
10	$C_{13}H_{18}O_2$	206.28	-656.250	-656.250	-656.311	2.113

9 show a higher free energy value of -1709.044 and -1713.412 Hartree respectively than the other analogues. When describing a molecule's electrical properties, it is crucial to consider its dipole moment value. A high value denotes a molecule's highly polar nature and, hence, higher intermolecular interactions. Additionally, it predicts the chemical composition and dielectric characteristics of any solvent.[40-42] Improved dipole moments in drug design can improve hydrogen bonds and non-bonded interactions in drug-receptor complexes, which play a crucial role in raising binding affinity.[43] Here, compound 7 has the highest value of dipole moment (7.066 Debye) due to the attachment of Oxygen (O) and Nitrogen (N) with the aromatic ring.

Molecular orbital analysis

Frontier molecular orbital theory states that the "Lowest Unoccupied Molecular Orbital (LUMO)" and "Highest Occupied Molecular Orbital (HOMO)" are important indicators of a molecule's chemical stability and reactivity, respectively.[44] The transition from the ground to the first excited state is related to the electronic absorption, which is mostly stated by a single excited electron from HOMO to LUMO.[45] Chemical qualities such as chemical hardness and softness, chemical potential, electronegativity, and electrophilicity are all based on the value of the HOMO-LUMO gap.[46,47] Larger HOMO-LUMO gaps are associated with reduced chemical softness and higher kinetic stability because the transfer of one electron from HOMO to LUMO occurs under energetically unfavorable circumstances.Due to the ease of electron transition, a lower HOMO-LUMO gap is linked to the upper chemical softness and lower kinetic stability.[48] From Table 2, among the compounds 2-9, the compound 5 has highest energy gap value (5.090 eV) and compound 4 has lowest energy gap value (2.150 eV) than that of other counterparts (Figure 3(a) and 3(b)). Compound 5 has the maximum chemical hardness and minimum softness value (2.545 eV) and (0.196 eV) respectively, whereas, compound 4 has the lowermost chemical hardness (1.075 eV) as well as the uppermost softness (0.465 eV) respectively, among the compounds 2-9. In overall, all tested heterocyclic aspirin 2-9 showed lower energy gap, chemical hardness as well as the higher chemical softness indicates their dominant chemical reactivity in compared to that of standard drugs aspirin (1) and ibuprofen (10).

Molecular electrostatic potential analysis

The total charge of the electrons and nuclei are shown on the molecular electrostatic potential (MEP) map, which also provides some information on the electronegativity, partial charge, dipole moment, and chemical reactivity of the molecule.[49,50] By using the colors blue and red, it depicts a potential electrophilic and nucleophilic attack.[51] Red color depicts maximum negative regions that are electron rich and have the potential for electrophilic attack. Because there are fewer electrons present, the deep blue color of the utmost positive region indicates that it may be a target for nucleophilic attack.[52] Furthermore, green color shows zero potential area. When it comes to color grading, MEP simultaneously displays molecule size, shape, and positive, negative, and neutral electrostatic potential portions. The area with the negative potential is over electronegative atoms (oxygen atoms) on the MEP map (Figure 4), whereas the region with the positive potential is over hydrogen atoms. Here, compound 2 shows the highest negative potential value (-7.124e-2 a.u., deepest red) and maximum positive potential value (+7.124e-2 a.u., deepest blue).

Vibrational frequencies analysis

In Table 3 and Figure 5, respectively, several IR vibrational frequencies and IR spectra are shown. The scaling factor 0.9648[53] is applied after calculating all vibrational frequencies in the gas phase at the same theoretical level.[54] The infrared (IR) spectra of all substances, which were measured between range of 400-4000 cm^{-1}, were used to identify the regions of absorption caused by the various functional groups. The band found in the region 3090 –3130 cm^{-1} is attributed to the aromatic νC-H stretching. The band observed between 1269 and 1428 cm^{-1} due to symmetric stretching of νC-N and another band in the region 835– 970 cm^{-1} is assigned to symmetric stretching of νN-N group. The band observed at 1142 cm^{-1} due to the symmetry stretching of νO-H for compound 8 and the band observed at 508 cm^{-1} confirms the presence of νC-S group. Band observed at 2446 cm^{-1} confirms the presence of νS-H group in compound 5. Aromatic νC-O stretch value for compound 7 found at 1639 cm^{-1}.

UV-visible spectroscopy analysis

For the molecular orbital study of fused aromatic ring systems, the Time-dependent density functional theory (TD-DFT) technique for UV-visible spectroscopy serves as a standard, ensuring a balance between accuracy and computing expense. In this study, the first electron transitions from the initial state (S_0) to singlet (S_1) depend on kinetic stability and reactive sites. The table 4 and figure 6 show each of the two distinctive electronic transition states of counterpart. Compound 7 and Compound 8 show large absorption bands at 731.28 nm and 677.60 nm together with their oscillator strengths 0.0180 and 0.0070. The highest wavelength of the configurations [(H→L)] for compound 7 and [(H→L)] for compound 8 is the consequence of the electron's charge transfer to the excited state $S_0 \rightarrow S_1$. The maximum intensities of the broadband absorption wavelengths at 731.28 nm and 677.60 nm are mostly caused by the electronic transition from HOMO to LUMO. Chemical reactivity is maximized, and kinetic stability is minimized by the lower excitation energy that corresponds to the HOMO-LUMO energy gap.[37] Since compounds 7 and Compound 8 have lower excitation energies 1.695 and 1.829 eV, respectively this implies they have more reaction sites. On the other hand, for the transition $S_0 \rightarrow S_1$, compound 1 and compound 10 have the fewest

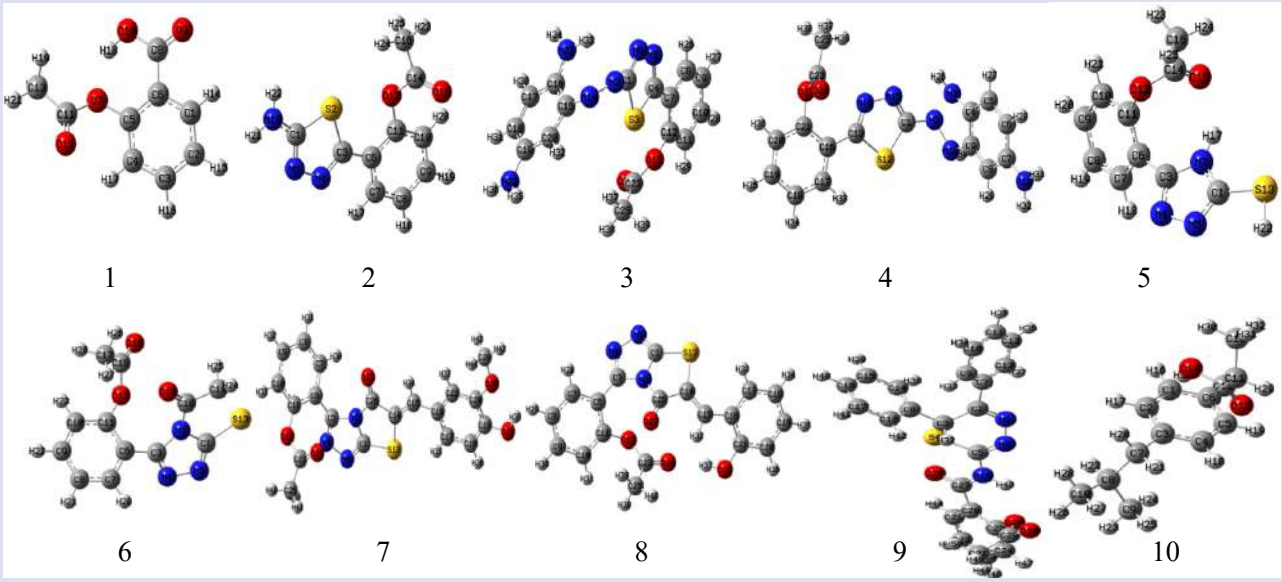

Figure 2: Optimized structures of all compounds 1-10.

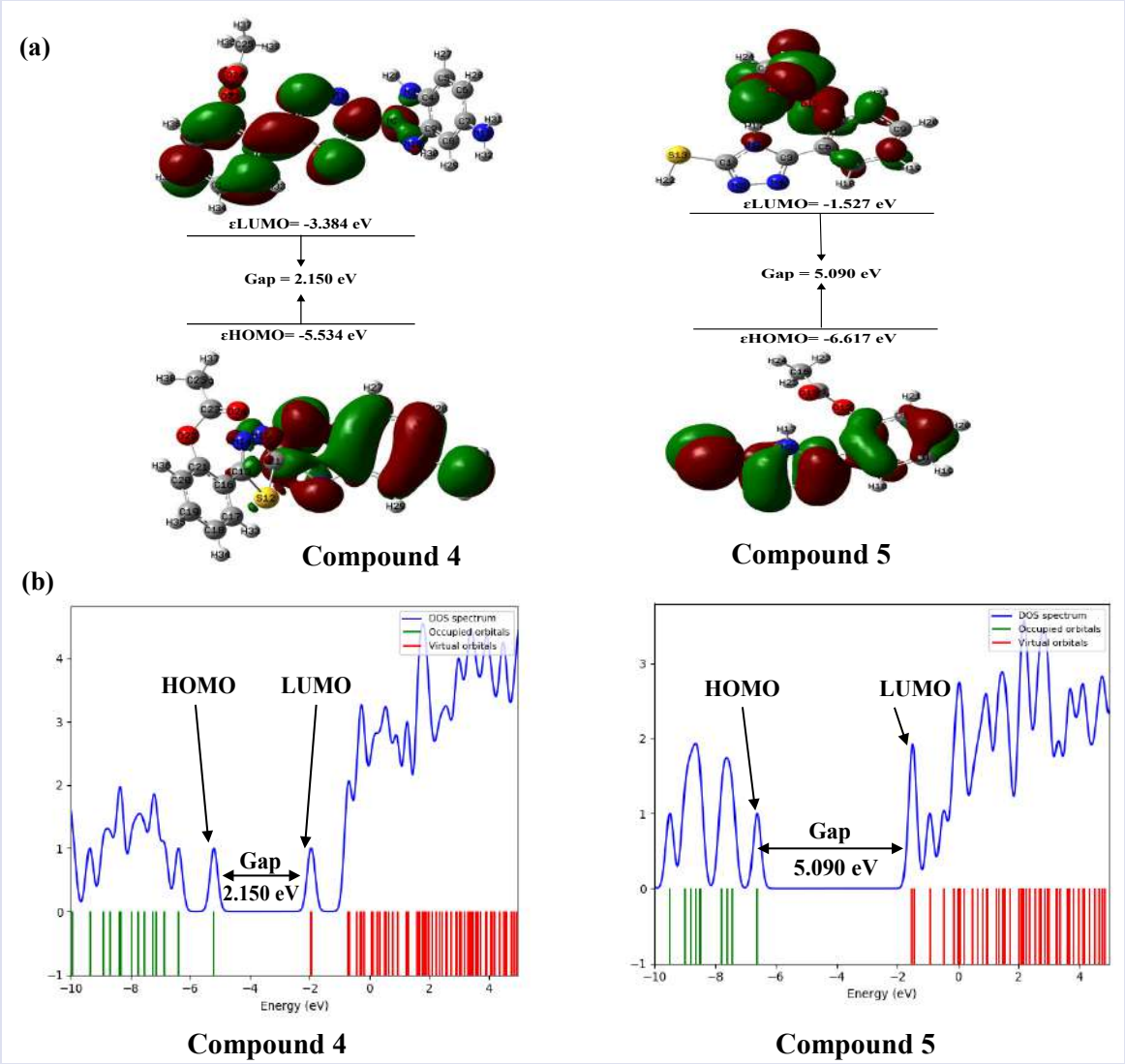

Figure 3: (a) HOMO-LUMO gap and (b) DOS plotof compound 4 and coumpound 5.

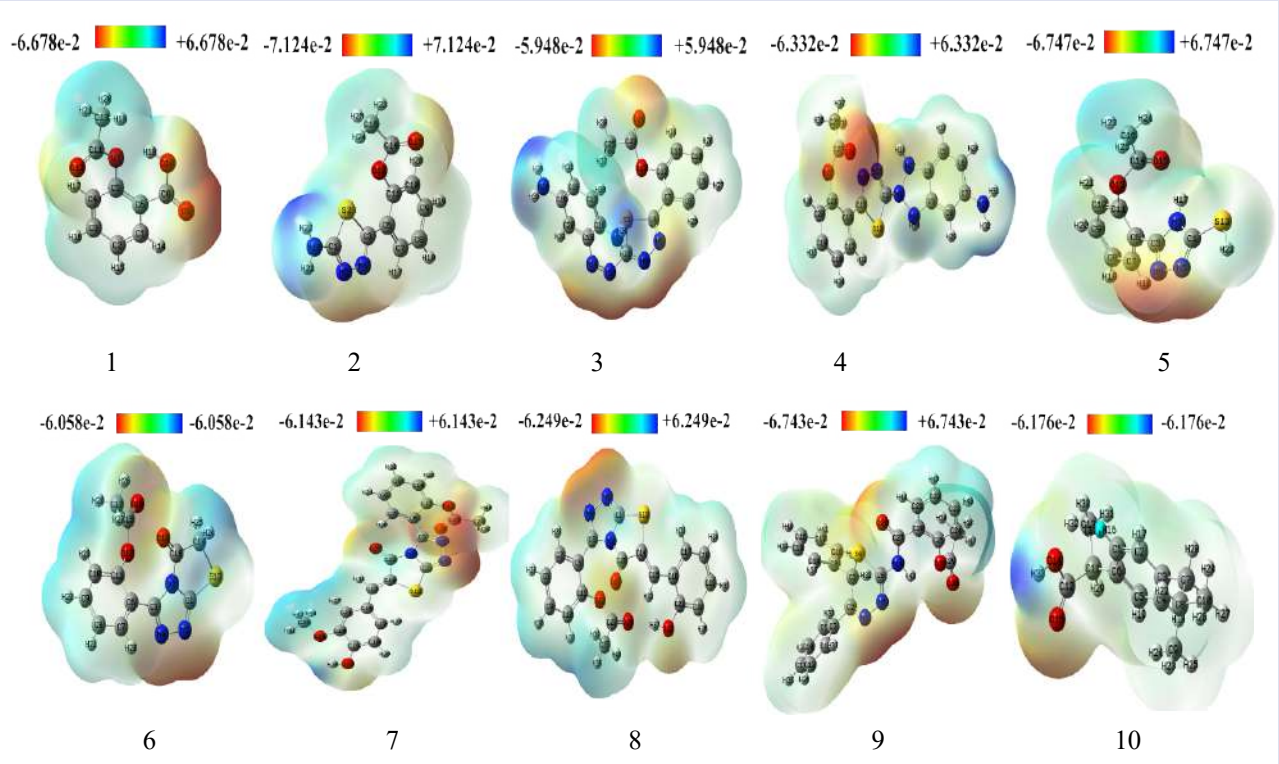

Figure 4: Molecular electrostatic potential map of all compounds 1-10.

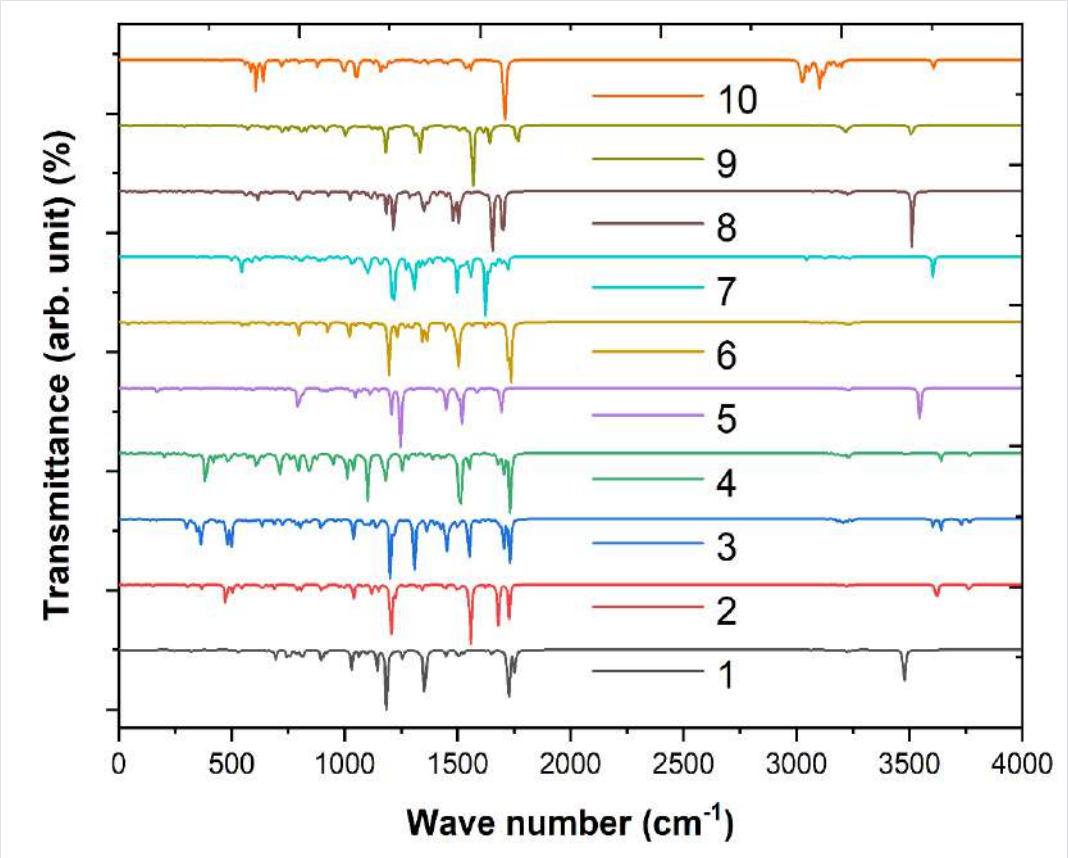

Figure 5: FT-IR spectroscopy of all studied compounds 1-10.

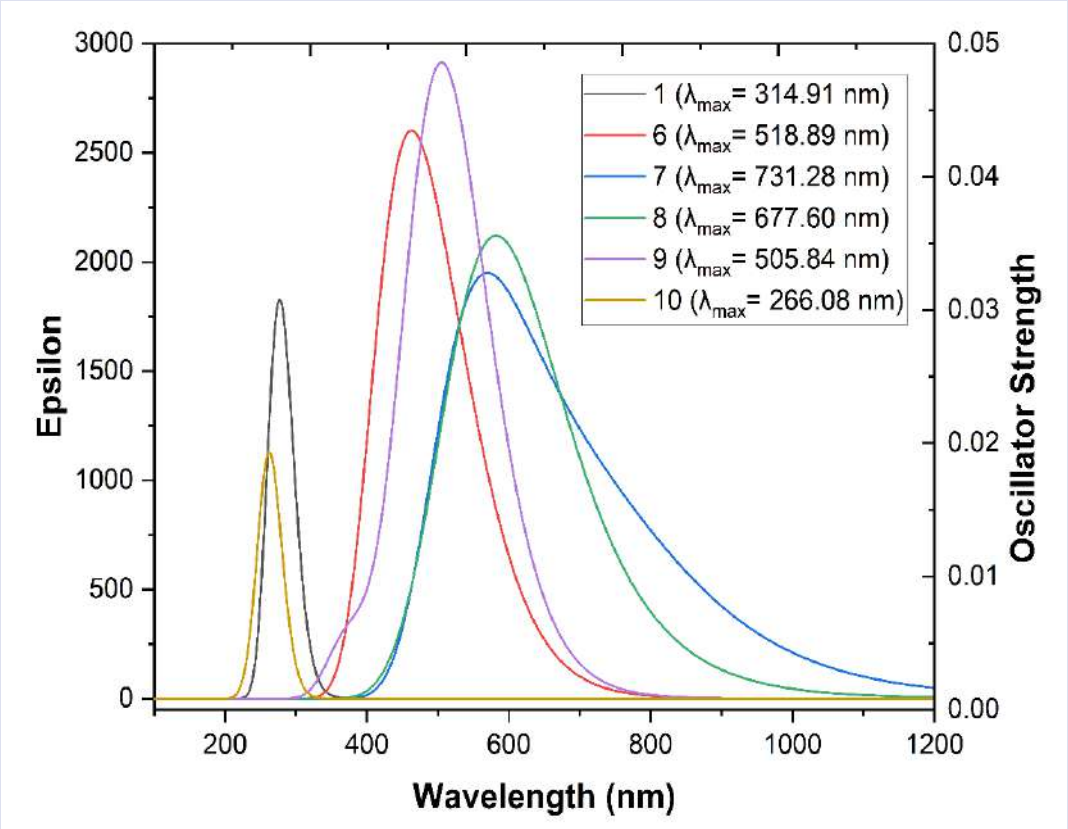

Figure 6: UV-visible spectroscopy of selected compounds.

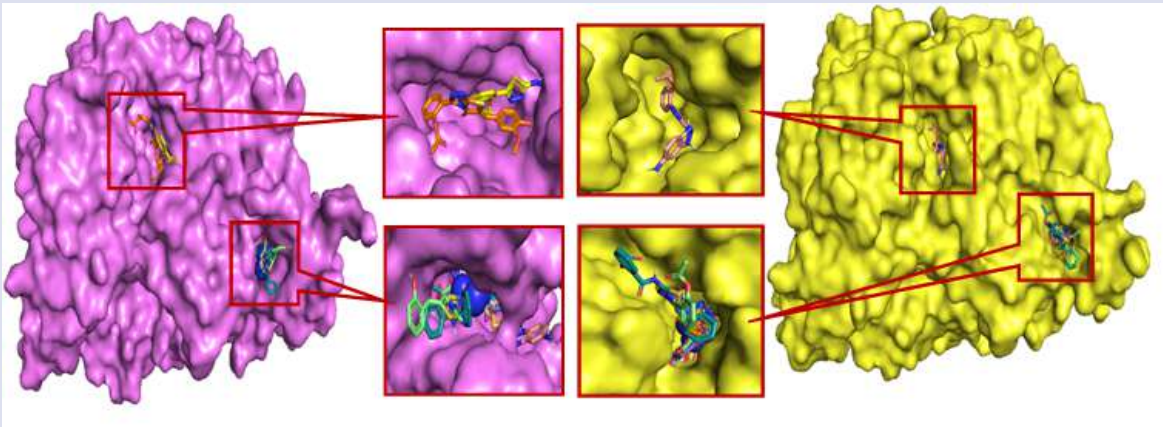

Figure 7: Docked conformer of all compounds at inhibition binding site of receptor protein (a) 6Y3C and (b) 5F19.

reaction sites with high excitation energy of 3.937 eV and 4.659 eV with tropical oscillator strength of 0.0002 and 0.0200. The other significant excited states exist in compounds 2, 4, 6, 9 having transition energies 3.388, 2.650, 2.389 and 2.451 eV respectively with moderate reactive sites. Here, compounds 2-9 have lower excitation energy compared to compounds aspirin (1) and ibuprofen (10). Hence compounds 2-9 show more reaction sites than drugs aspirin (1) and ibuprofen (10).

Molecular docking and interaction calculation

The charge and/or the potentiality of the receptor protein's nature is characterized by electrostatic potential map, which may assist in determining the ligands' binding modes. Molecular docking is the processes of two or more molecules interacting to form a stable adduct, and it is an important task as in hit detection, lead optimization, bioremediation, and rational drug design processes.[56] As in approach, computer-based biomolecular docking and novel lab-based procedures would complement each other for the establishment of esoteric bioactive compounds.[57] However, negative binding affinity values indicate a stronger interaction here between compounds and the receptor proteins (Figure 7a and 7b). The binding of the structures of the investigation is linked to non-covalent interactions such as hydrogen bonds, halogen bonds, and hydrophobic interactions (Table 5a and 5b) and these interactions can boost the binding affinity at the drug-receptor interface and also serve to stabilize the ligands at the target sites, which influences binding affinity and drug effectiveness.[58] Strong hydrogen bonding with less than 2.3 Å, however, is subjected to

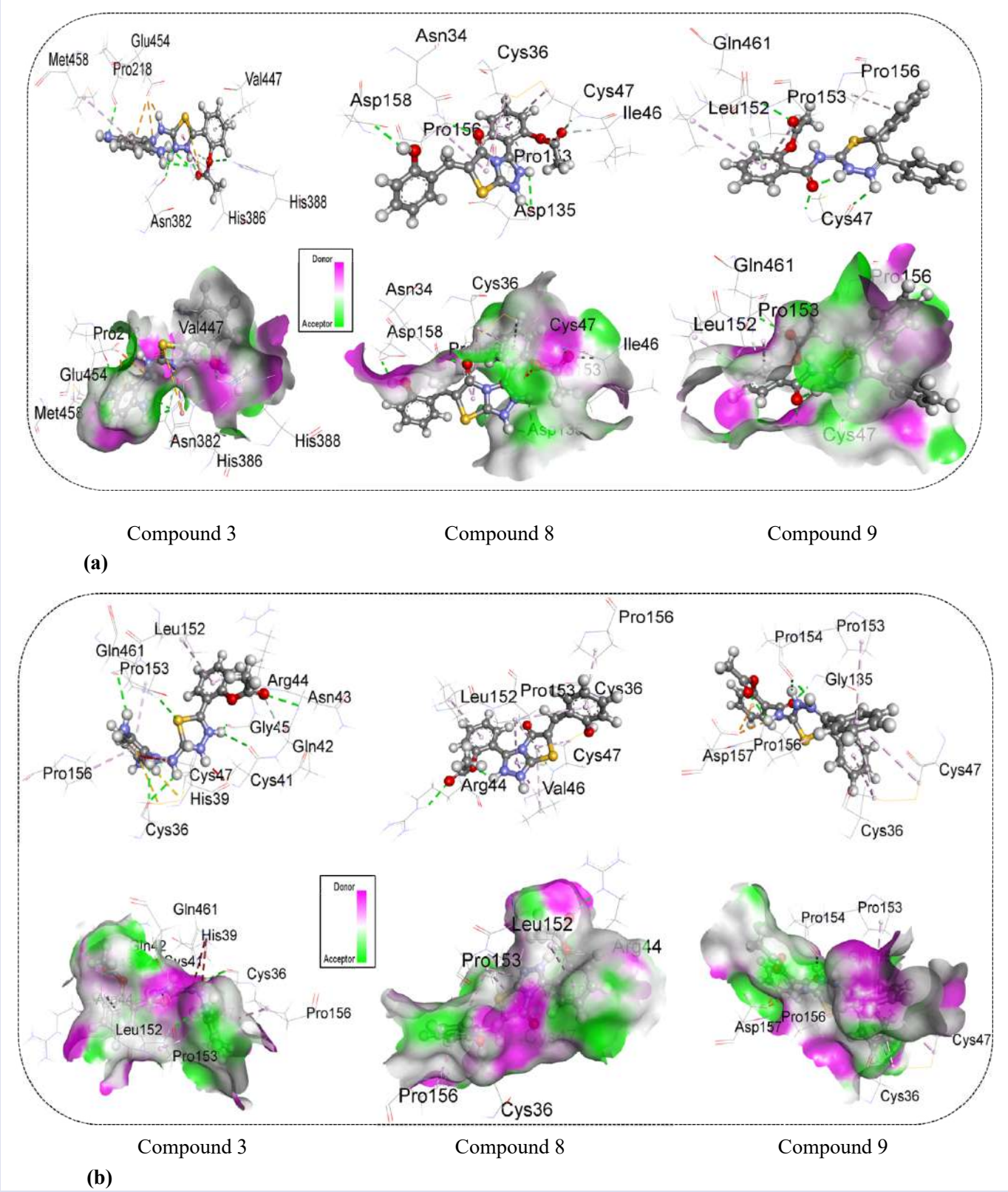

Figure 8: Non-bonding interactions and hydrogen bond surface of selected compounds with (a) 6Y3C and (b) 5F19.

Table 2: Energy (eV) of HOMO-LUMO, gap, hardness (η), softness (S), chemical potential (μ), electronegativity (χ), and electrophilicity (ω) of investigated compounds 1-10.

Compound	εHOMO	εLUMO	Gap	η	S	μ	χ	ω
1	-7.685	-2.138	5.547	2.77	0.180	-4.911	4.911	4.353
2	-6.245	-1.826	4.419	2.209	0.226	-4.035	4.035	3.685
3	-5.363	-2.975	2.388	1.194	0.418	-4.169	4.169	7.278
4	-5.534	-3.384	2.150	1.075	0.465	-4.459	4.459	9.248
5	-6.617	-1.527	5.090	2.545	0.196	-4.072	4.072	3.257
6	-6.991	-2.577	4.414	2.207	0.226	-4.784	4.784	5.185
7	-6.339	-3.008	3.331	1.665	0.300	-4.673	4.673	6.559
8	-6.552	-3.059	3.493	1.746	0.286	-4.805	4.805	6.611
9	-6.283	-2.359	3.924	1.962	0.254	-4.321	4.321	4.758
10	-6.681	-0.946	5.735	2.865	0.174	-3.813	3.813	2.538

Table 3: Selected vibrational frequencies (cm^{-1}) of studied compounds (1-10) calculated in gas phase (scaled).

Compound	Assignment	Vibrational frequencies (cm^{-1})	Vibrational frequencies (cm^{-1})
		Initial	Scaled
1	νC-C^a stretch	1643	1585
	νC-N stretch	1315	1269
	νN-Hstretch	3567	3441
	νC-Hstretch	3241	3127
	νC-C^b stretch	1127	1087
2	νC-C^a stretch	1662	1603
	νC-H^b stretch	3042	2935
	νC-H^a stretch	3204	3091
4	νC-C^a stretch	1506	1453
	νC-C^a stretch	1651	1593
	νC-H^b stretch	3641	3513
	νC-H^a stretch	3203	3090
	νN-N^a stretch	943	910
5	νC-C^a stretch	1664	1605
	νC-H^b stretch	1447	1396
	νC-H^a stretch	3241	3127
	νS-H^b stretch	2535	2446
	νN-N^a stretch	991	956
6	νC-O^b stretch	1233	1190
	νC-H^b stretch	1449	1398
	νC-H^a stretch	3242	3128
	νC-C^a stretch	1624	1567
	νC-N^a stretch	1498	1445
7	νC-C^a stretch	1620	1563
	νC-H^b stretch	3046	2939
	νC-O^a stretch	1699	1639
	νN-N^a stretch	865	835
8	νC-C^a stretch	1610	1553
	νO-H^b stretch	1184	1142
	νC-S^a stretch	527	508
	νC-C^{b}stretch	1447	1396
	νC-N^a stretch	1480	1428
9	νN-N^a stretch	1001	966
	νC-C^a stretch	1651	1593
	νC-H^b stretch	1089	1051
	νC-H^a stretch	877	846
	νC-N^a stretch	1544	1490
10	νC-H^b stretch	1458	1407
	νC-H^b stretch	3031	2924
	νC-C^a stretch	1660	1602
	νC-O^a stretch	1709	1649

* a = aromatic, b = aliphatic

Table 4: Electronic absorption spectra of all tested compounds 1-10. Calculated at TD-DFT/ B3LYP/ 6-31G+.

Compound	Excited state	Wavelength (nm)	Excitation energy (eV)	Configurations composition	Oscillator strength
1	$S_0 \rightarrow S_1$	314.91	3.937	0.654(H-1 →L), -0.151(H-1 →L+1), 0.101(H-1 →L+5), 0.159(H+1 →L)	0.0002
	$S_0 \rightarrow S_2$	283.98	4.366	0.208(H-3 →L), 0.321(H-3 →L+1), -0.119(H-2 →L+2), -0.112(H-1 →L), 0.488(H →L), 0.262(H →L+1)	0.0170
2	$S_0 \rightarrow S_1$	365.91	3.388	0.141(H-2→L), 0.664(H→L), 0.104(H→L+2),	0.0160
	$S_0 \rightarrow S_2$	311.08	3.985	-0.198(H-4→L), 0.203(H-3→L), 0.170(H-2→L), 0.579(H-1→L)	0.0140
3	$S_0 \rightarrow S_1$	870.07	0.432	0.702(H→L)	0.0003
	$S_0 \rightarrow S_2$	796.75	1.556	0.534(H-2→L), 0.446(H-1→L), 0.101(H→L)	0.0030
4	$S_0 \rightarrow S_1$	467.90	2.650	0.699(H→L)	0.0221
	$S_0 \rightarrow S_2$	413.41	2.999	0.698(H→L+1)	
5	$S_0 \rightarrow S_1$	282.21	4.393	-0.161(H-5→L+1), 0.144(H-4→L), -0.364((H-4→L+1), -0.126(H-4→L+3), 0.213(H→L), 0.448(H→L+1), 0.150(H→L+3)	0.0010
	$S_0 \rightarrow S_2$	270.25	4.587	0.124(H-5→L), 0.614(H-1→L), -0.131(H-1→L+1), -0.111(H-1→L=2), -0.226(H→L)	0.0010
6	$S_0 \rightarrow S_1$	518.89	2.389	0.662(H→L), -0.232(H→L+1)	0.0262
	$S_0 \rightarrow S_2$	451.82	2.744	0.229(H→L), 0.663(H→L+1)	0.0425
7	$S_0 \rightarrow S_1$	731.28	1.695	0.696(H→L)	0.0180
	$S_0 \rightarrow S_2$	560.59	2.211	0.693(H-1→L)	0.0390
8	$S_0 \rightarrow S_1$	677.60	1.829	0.697(H→L)	0.0070
	$S_0 \rightarrow S_2$	580.91	2.134	0.693(H-1→L)	0.0450
9	$S_0 \rightarrow S_1$	505.84	2.451	0.667(H→L), 0.159(H→L+1)	0.0716
	$S_0 \rightarrow S_2$	402.59	3.080	-0.182(H→L), 0.669(H→L+1)	0.0037
10	$S_0 \rightarrow S_1$	266.08	4.6596	0.432(H-2→L), 0.132(H-1→L), 0.532(H→L)	0.0200
	$S_0 \rightarrow S_2$	254.56	4.8705	0.534(H-2→L), -0.444(H→L)	0.0089

Table 5(a): Binding affinity and non-bonding interactions of studied compounds 1-10 with COX-1(6Y3C).

Compound	Binding Affinity (Kcal/mol)	Residue in Contact	Interaction Type	Distance (Å)
1	-6.1	HIS43	H	2.76964
		GLN44	H	2.10788
		GLN461	H	1.96000
		TYR39	CHy	2.86344
		LEU152	PA	4.67661
		PRO153	PA	5.38319
2	-6.5	CYS47	H	2.08321
		TYR130	H	2.86377
		CYS47	H	3.06341
		CYS47	H	1.87499
		ILE46	CHy	2.59531
		CYS36	PA	4.55543
		CYS47	PA	5.25424
		PRO153	PA	5.14945
		CYS36	PA	4.97750
		CYS47	PA	4.40599
		PRO153	PA	4.21447
3	-8.4	GLU454	PC	1.92347
		GLU454	PC	3.26826
		HIS388	H	2.97462
		ASN382	H	2.57780
		HIS386	H	2.74240
		PRO218	H	2.62000
		HIS386	H	2.50766
		HIS386	CHy	2.85657
		GLU454	Pa	3.91292
		HIS386	PSu	5.12053
		HIS386	PPTSh	4.81465
		MET458	PA	5.49464
		VAL447	PA	4.16510

		CYS47	H	2.75033
		CYS41	H	2.00270
		PRO156	CHy	2.62118
		GLU465	Pa	4.90931
		CYS36	PSu	4.44007
4	-8.7	CYS41	PSu	5.65868
		CYS36	A	4.57376
		PRO156	A	5.42843
		CYS47	PA	4.28412
		PRO153	PA	4.33449
		LEU152	PA	5.43454
		CYS47	H	2.31878
		CYS36	H	2.80991
		CYS36	H	2.32992
		TYR39	PSu	5.65490
		CYS36	PA	4.69957
5	-6.6	CYS47	PA	4.05965
		PRO153	PA	5.25424
		CYS36	PA	4.89368
		CYS47	PA	5.25311
		PRO153	PA	4.02656
		TYR130	H	2.34060
		GLN461	H	2.92046
		CYS47	H	2.62224
		ILE46	Chy	2.79550
6	-7.4	PRO153	Chy	2.50432
		CYS47	PA	4.18239
		PRO153	PA	3.98787
		CYS41	PA	4.88076
		GLN203	H	2.54901
		GLN203	H	2.22225
		THR212	H	2.30059
		HIS388	H	2.41746
		PHE210	H	2.94965
7	-8.0	HIS388	PC	4.92581
		MET391	PSu	5.49477
		VAL447	PA	4.35968
		VAL447	PA	4.64440
		ILE444	PA	4.58380
		ASN34	H	2.32498
		CYS47	H	2.05776
		ASP135	H	2.26077
		ASP158	H	2.52262
		PRO125	H	5.38057
8	-8.2	CYS36	PA	5.27379
		PRO156	PA	5.30100
		CYS36	PA	4.33879
		CYS47	PA	4.79449
		PRO153	PA	4.34141
		PRO156	PA	5.34739
		CYS47	H	2.09089
		GLN461	H	2.57027
		CYS47	H	2.45557
9	-9.1	GLN461	Pd	2.97287
		LEU152	PA	5.43881
		PRO153	PA	4.59364
		PRO156	PA	4.63750
		GLN44	H	2.34129
		GLN461	Pd	2.99052
		LEU152	A	4.95196
		CYS36	A	4.25432
10	-6.6	PRO153	A	4.40660
		PRO156	A	4.60417
		TYR39	PA	4.75142
		LEU152	PA	5.27474
		PRO153	PA	5.02419

H = Conventional Hydrogen Bond, A = alkyl, PA = Pi-alkyl, PC = Pi-cation, Pa = Pi-anion, X = Halogen bond, CHy = Carbon Hydrogen Bond, Pd = Pi-donor, PS = Pi-sigma, PSu = Pi-sulfur, PPS = Pi-Pi stacked, PPTSh = Pi-Pi T-shaped, APS = Amide-Pi stacked.

Table 5(b): Average Binding affinity and non-bonding interactions of investigated compounds 1-10 with receptor protein 5F19 (COX-2).

Compound	Binding Affinity (Kcal/mol)	Residue in Contact	Interaction Type	Distance (Å)
1	-6.2	TYR385	H	2.88129
		ALA527	CHy	2.76449
		OAS530	CHy	2.88612
		VAL349	PA	5.39680
		LEU352	PA	4.62783
		VAL523	PA	4.51377
		ALA527	PA	5.01156
2	-7.3	ARG44	H	2.01108
		CYS47	H	2.85355
		CYS36	H	2.89085
		CYS36	H	2.79095
		ARG44	CHy	2.91648
		CYS47	PA	5.48850
		PRO153	PA	4.60569
		ARG44	PA	5.24582
		LEU152	PA	5.39415
		PRO153	PA	5.10040
3	-8.9	ASN43	H	2.79227
		ARG44	H	1.97348
		GLN461	H	2.78505
		CYS36	H	2.48118
		CYS41	H	2.69571
		GLY45	H	2.70378
		CYS36	H	2.89210
		PRO153	H	2.68899
		CYS36	H	2.94923
		CYS47	H	2.31156
		GLN42	CHy	2.93519
		ARG44	PS	2.89676
		CYS36	PSu	5.07273
		CYS47	PSu	5.76804
		PRO153	PA	4.91591
		PRO156	PA	4.67401
		LEU152	PA	5.06809
4	-7.9	TYR130	H	2.86886
		LYS137	H	2.87806
		LYS137	H	2.47541
		ASP125	H	2.28780
		CYS41	H	2.15204
		ASP125	Pa	3.46330
		TYR130	PSu	5.47789
		ARG44	PA	4.59084
		ARG44	PA	5.15450
		LEU152	PA	5.31101
5	-6.9	CYS41	H	2.82309
		GLY45	H	2.36064
		CYS36	H	3.05794
		ARG44	CHy	2.15111
		CYS47	PSu	5.94305
		HIS39	PSu	4.75873
		CYS41	PA	4.83537
		LEU152	PA	4.70147
		ARG469	PA	5.09227
6	-7.8	ARG44	H	2.52421
		GLN461	H	2.86221
		GLN461	H	2.26941
		GLU465	H	2.48000
		HIS39	CHy	2.25698
		ARG44	Chy	2.01715
		GLU465	PSu	3.31521
		LEU152	PA	4.56377
		VAL46	PA	5.28115
		PRO153	PA	4.22783

		CYS36	H	2.57256
		GLY135	CHy	2.47517
		ARG469	CHy	2.86335
		HIS39	PSu	4.48148
		GLY135	APS	4.07665
		CYS36	PA	5.01813
		CYS36	PA	4.06088
7	-8.5	CYS47	PA	4.59560
		CYS47	PA	4.82565
		PRO153	PA	4.39092
		PRO153	PA	5.37213
		PRO156	PA	4.61975
		LEU152	PA	5.36071
		CYS36	PA	5.0686
		ASN34	H	2.54691
		PRO154	H	2.21506
		CYS47	H	3.00400
		CYS47	Pd	2.81837
		GLY135	PS	2.62811
8	-8.7	PRO156	PS	2.58860
		TYR136	PPTSh	4.99637
		VAL155	APS	5.23075
		VAL46	PA	5.15946
		CYS47	PA	5.13559
		PRO153	PA	4.20194
		ASP157	H	2.70811
		GLY135	H	2.10443
		PRO154	H	3.03248
		PRO154	H	1.93890
		TYR134	CHy	2.89556
9	-9.4	ASP157	PA	3.35047
		CYS36	PA	4.75768
		CYS36	PA	4.58523
		CYS47	PA	5.09345
		PRO153	PA	4.71476
		PRO156	Pa	5.01788
		TYR385	H	2.55961
		GLY526	CHy	3.07839
		ALA527	A	3.76693
		MET522	A	4.56606
		VAL349	A	4.83534
		LEU359	A	4.50264
		TYR355	PA	4.77832
10	-7.0	TYR355	PA	5.19732
		TRP387	PA	5.05174
		PHE518	PA	4.26001
		VAL349	PA	5.06936
		LEU352	PA	4.90531
		VAL523	PA	4.70468
		ALA527	PA	4.65942

H = Conventional Hydrogen Bond, A = alkyl, PA = Pi-alkyl, PC = Pi-cation, Pa = Pi-anion, X = Halogen bond, CHy = Carbon Hydrogen Bond, Pd = Pi-donor, PS = Pi-sigma, PSu = Pi-sulfur, PPS = Pi-Pi stacked, PPTSh = Pi-Pi T-shaped, APS = Amide-Pi stacked.

Table 6: Pharmacokinetic parameters of aspirin (1), heterocyclic aspirin derivatives (2–9) and ibuprofen (10).

Compound	Absorption			Distribution		Metabolism		Toxicity			
	HIA	HOB	C2P	BBB	P-GpI /P-GpS	CYP3A4I / CYP3A4S	CYP4502C9I / CYP4502C9S	hERG	Carcinogen	AOT	RAT LD_{50} (mol/Kg)
1	+0.965	+0.85	+0.661	+0.938	NI (0.962) / NS (0.685)	NI (0.961) / NS (0.722)	NI (0.907) / NS (0.752)	WI (0.943)	NC (0.836)	II (0.726)	2.639
2	+1.000	+0.55	+0.513	+0.916	NI (0.971) / NS (0.815)	NI (0.876) / NS (0.669)	I (0.688) / NS (0.833)	WI (0.942)	NC (0.872)	III (0.513)	2.409
3	+0.991	+0.55	+0.576	+0.770	NI (0.986) / S (0.734)	NI (0.763) / NS (0.517)	NI (0.609) / NS (0.622)	WI (0.965)	NC (0.833)	III (0.563)	2.610
4	+0.979	+0.55	+0.545	+0.710	NI (0.987) / NS (0.703)	NI (0.601) / NS (0.647)	I (0.688) / NS (0.759)	WI (0.929)	NC (0.807)	III (0.602)	2.410
5	+1.000	+0.55	+0.541	+0.899	NI (0.967) / NS (0.747)	NI (0.807) / NS (0.697)	I (0.746) / NS (0.775)	WI (0.971)	NC (0.884)	III (0.485)	2.402
6	+1.000	+0.55	+0.552	+0.780	NI (0.966) / NS (0.757)	NI (0.733) / NS (0.557)	NI (0.500) / NS (0.763)	WI (0.992)	NC (0.809)	III (0.562)	2.579
7	+0.675	+0.55	+0.546	+0.723	NI (0.586) / NS (0.575)	NI (0.869) / S (0.570)	NI (0.509) / NS (0.758)	WI (0.993)	NC (0.876)	III (0.553)	2.694
8	+0.993	+0.55	+0.542	+0.639	NI (0.975) / NS (0.645)	NI (0.513) / NS (0.508)	I (0.608) / NS (0.603)	WI (0.991)	NC (0.804)	III (0.585)	2.515
9	+0.665	+0.55	+0.580	+0.788	NI (0.958) / S (0.698)	NI (0.597) / NS (0.524)	NI (0.531) / NS (0.714)	WI (0.996)	NC (0.648)	III (0.567)	2.588
10	+0.993	+0.85	+0.887	+0.962	NI (0.932) / NS (0.759)	NI (0.966) / NS (0.688)	NI (0.931) / NS (0.759)	WI (0.972)	C (0.555)	III (0.808)	2.309

HIA=Human intestinal absorption, HOB=Human oral bio availability, C2P=CACO-2 permeability, BBB=Blood brain barrier, *p*-GpI=*p*-glyco-protein inhibitor, *p*-GpS=*p*-glyco-protein substrate, hERG=human ether-a-go go related gene, AOT=Acute oral toxicity, RAT=Rat acute toxicity, S=Substrate, NS=Non-substrate, I=Inhibitor, NI=Non-inhibitor, WI= Weak inhibitor, NC=Non-carcinogen, C=Carcinogen, CYP3A4*I*=CYP3A4 Inhibition, CYP3A4*S* = CYP3A4 Substrate.

Table 7: QSAR parameters of investigated compounds 1-10.

Compound	Chiv5	bcutm1	MRVSA9	MRVSA6	PEOEVSA5	GATSv4	J	Diametert	pIC_{50}
1	0.521	3.848	11.939	29.829	12.133	1.011	2.462	6.0	4.0214
2	1.156	4.230	22.438	24.265	23.470	1.045	1.930	8.0	4.6166
3	1.207	4.024	25.345	32.837	23.470	0.805	1.806	11.0	4.4631
4	1.838	4.237	39.500	42.465	23.470	1.081	1.456	13.0	4.5800
5	0.910	4.001	18.598	24.265	12.133	0.902	1.930	8.0	4.2527
6	1.215	4.024	23.456	27.312	12.133	0.706	1.815	10.0	4.3817
7	3.208	4.457	22.374	62.914	34.218	0.937	1.301	13.0	5.5137
8	4.564	4.269	32.450	56.345	34.212	0.881	1.205	13.0	5.4846
9	8.454	4.975	37.238	90.028	0.000	1.063	1.184	14.0	6.4302
10	0.925	3.861	5.969	35.392	38.113	1.010	2.291	9.0	6.6181

significantly increase the binding affinity.[59] However, the common types of interactions found in this study are hydrogen, carbon-hydrogen, π-alkyl, π-sulfur and π-π T-shaped. Non-covalent interactions engaging π systems are crucial to biological processes including the recognition of ligand-protein.[60] The binding affinity value found in the docking study, of compound 9 with receptor protein 5F19 is -9.4 kcal/mol, which is the highest among all the other compounds and this value of compound 3 and compound 8 are -8.9 kcal/mol and -8.7 kcal/mol, respectively, are also high because of strong hydrogen bond with ARG44 and PRO154 with a distance of 1.97348 Å and 2.21506 Å, respectively (Figure 8(a)). On the other hand, the value of binding affinities of compound 1 (-6.2 kcal/mol) and compound 5 (-6.9 kcal/mol) are relatively lowest, which means their less attraction towards the protein. Again, in case of protein 6Y3C, the binding interaction value of compound 9 (-9.1 kcal/mol) and compound 4 (-8.7 kcal/mol) are the highest among every studied compounds and the presence of strong hydrogen bonds with CYS47 and CYS41 with a distance of 2.09089 Å and 2.00270 Å, respectively, support the result (Figure 8(b)). The binding affinity of compound 1 (-6.1 kcal/mol) and compound 2 (-6.5 kcal/mol) are the lowest among the compounds with the protein 6Y3C. More importantly, all the examined derivatives 2-9 showed comparatively higher binding affinities with COX-1 and COX-2 protein than that of aspirin (1) and ibuprofen (10). The remaining compounds except compound 1, 6 and 10 in case of protein 5F19 and compounds 1, 3 and 7 in case of protein 6Y3C interact with CYS41 and CYS47 with π-alkyl bonding and π-sulfur bonding in place of hydrogen bond demonstrating that cysteine is the common residue which interacts with all the compounds. π-alkyl interactions are found in almost all the compounds with both proteins with the LEU352, LEU152, PRO153, VAL523, ALA527, ARG44, VAL46, TYR355, TRP387, VAL447, ILE444, PRO156, TYR39 residues. Amide-π stacked and π-π stacked are found with GLY135, VAL155 and TYR136, HIS386, respectively, which are also important as they contribute to the higher binding affinity. Furthermore, our investigated derivatives show higher affinity towards COX-2 protein than COX-1. It is evident that these derivatives can work better against COX-2.

ADMET analysis

ADMET stands for "absorption, distribution, metabolism, excretion, and toxicity". ADMET assesses all potential pharmacological properties which is essential in the development of drugs.[61] ADMET characteristics of heterocyclic aspirin analogues (2–9) are reported in Table 6 by the online *admetSAR* database. *AdmetSAR* data (Table 6) showed that all compounds 2–9 respond positively to human intestinal absorption (HIA), and it's likely that nothing can be eliminated from the body more quickly through the urinary and rectal systems.[62] Here, compounds 2, 5, and 6 exhibited more positive HIA (+1.000) response than aspirin (1) (+0.965) and also standard ibuprofen (10) (+0.993). All compounds showed positive HOB (human oral bioavailability) levels. In humans, positive oral bioavailability can result in health problems.[63] The human colon cancer cell line Caco-2 is propagated on permeable supports, and the permeability coefficients across the monolayers are used frequently to forecast the absorption of xenobiotics and other drugs taken orally.[64,65] In our study, all analogues 2–9 exhibited positive C2P values which indicate the rapid absorption of the drugs in human body as like as aspirin (1) and standard ibuprofen (10). The blood-brain barrier (BBB), an extremely constrictive barrier, closely regulates the movement of chemicals, electrolytes, and cells between the brain and the other regions of the body. This barrier protects the central nervous system from poisons, infections, inflammation, injury, and disease.[62,66] According to our analysis, each analog had a positive reaction to BBB, which is concerning and indicates that they will not pass BBB very rapidly. In blood brain barrier (BBB) results (Table 6), compound 2 and 5 showed comparatively better positive values than others which are +0.916 and +0.899, respectively. The removal of drugs received in the intestine and returned into the gut lumen is the primary method by which *p*-glycoprotein protects the body against hazardous substances.[59] *p*-glycoprotein can be blocked by obstructing drug-binding sites, preventing ATP hydrolysis, or changing the integrity of cell membranes.[67] The positive *p*-glycoprotein non-inhibition values of all heterocyclic aspirin derivatives (2-9) metabolites indicate that no one has an affinity for *p*-glucosylphosphorus.[68] A characteristic of a chemical's "pharmaceutical profiling" in drug modeling is the forecasting of *p*-glycoprotein substrate specificity (SPGP).[69] Here, compound 3 and 9 showed *p*-glycoprotein substrate activity. All compounds have no inhibition to CYP3A4 enzyme whereas only the compound 7 showed the substrate inhibition. A major cytochrome P450 enzyme called CYP2C9 was the target of drugs 2, 4, 5, and 8 that demonstrated inhibition. Inhibition affects many adverse drug interactions which are incorporated with the enzyme.[70,71] All of the compounds under investigation weakly inhibit the ether-a-go-go gene (hERG) in humans, which raises the danger of the long QT syndrome and other cardiac adverse effects like sudden death.[60,72] The detrimental effects of a substance on people as well as other living things *via* multiple biochemical systems are referred to as acute toxicity. A study on the threat of a substance's toxicological effects needs to take into account factors including acute oral, epidermal, and inhalation rodent toxicity.[73,74] Our research focused that, in comparison to aspirin (1), which exhibits acute oral toxicity, type II, all of the compounds 2–9 showed acute oral toxic effects (AOT) in class III, making them less harmful. A typical statistic used to categorize chemicals in terms of the potential risk they represent to human health following an initial exposure is the median lethal dosage for rodent oral acute toxicity (LD_{50}).[75,76] Here, all of the investigated heterocyclic aspirin derivatives (2–9) predicted LD_{50} were quite risky lying at 2.402-2.610mol/kg.

pIC_{50} studies

In order to study pIC_{50} values, the multi-linear regression (MLR) equation is applied. The relationship between a dependent variable (pIC_{50}) and a group of independent factors (descriptors Chiv5,

bcutm1, MRVSA9, MRVSA6, PEOEVSA5, GATSv4, J, and Diametert) are investigated using a MLR equation. According to Table 7, the pIC_{50} fluctuates between 4.0214 to 6.6181. It is stated that the pIC_{50} range for many drugs is 4.0-10. All of the compounds that were investigated in our study exhibited remarkable pIC_{50} values within the typical range of drugs.

CONCLUSION

In this study, the physicochemical as well as cyclooxygenase inhibition action of heterocyclic aspirin derivatives (2–9) were investigated. The structures 2–9 were supported by the calculations of equilibrium geometries, vibrational frequency, and UV–visible spectral data. All of the molecules under study have shown thermal stability, had lower HOMO-LUMO gaps, and also had a greater flexibility than the parent molecule. In compared to their parent drugs, most analogues have stronger non-bond interactions and binding affinities. Compared to COX-1 (6Y3C), all heterocyclic aspirin analogues 2–9 have better binding affinities with the COX-2 (5F19) protein. Furthermore, the 9–5F19 complex has a higher affinity for binding than other compounds due to the inclusion of both a polar acetate group (-$OCOCH_3$) and an amide functional group (-NH-CO-). Since all of the heterocyclic aspirin analogues showed acute toxicity in the level III category and had better pharmacokinetic features than aspirin (1), it is likely that they had better oral absorption capabilities. In light of the mentioned research, these findings may be beneficial in developing possible COX-2 inhibitors.

ACKNOWLEDGEMENTS

Authors are thankful to the Department of Drug Design, Computer in Chemistry and Medicine Laboratory, Dhaka, Bangladesh for their continuous support and suggestions.

CONFLICTS OF INTERESTS

Authors assert that there are no competing demands.

FUNDING

This research did not receive any external funding.

REFERENCES

1. Szczeklik, A., Gryglewski, R. J. & Czaizniawska-Mysik, G. Relationship of Inhibition of Prostaglandin Biosynthesis by Analgesics to Asthma Attacks in Aspirin-sensitive Patients. Br Med J. 1975;1(5949): 67–69. https://doi.org/10.1136/bmj.1.5949.67
2. Li, J. Y. et al. Synthesis of aspirin eugenol ester and its biological activity. Medicinal Chemistry Research. 2012;29(1): 995–999. https://doi.org/10.1007/s00044-011-9609-1
3. Vane, J. & Botting, R. Inflammation and the mechanism of action of anti-inflammatory drugs. The FASEB Journal. 1987;1(2):89–96. https://doi.org/10.1096/fasebj.1.2.3111928
4. Patrono, C. Aspirin and human platelets: from clinical trials to acetylation of cyclooxygenase and back. Trends Pharmacol Sci. 1989;10(11):453–458. https://doi.org/10.1016/S0165-6147(89)80010-0
5. Wallenburg, H. C. S., Makovitz, J. W., Dekker, G. A. &Rotmans, P. Low-Dose Aspirin Prevents Pregnancy-Induced Hypertension and Pre-Eclampsia in Angiotensin-Sensitive Primigravidae. The Lance, t. 1986;327(8471):1–3. https://doi.org/10.1016/S0140-6736(86)91891-X
6. Sostres, C. & Lanas, A. Gastrointestinal effects of aspirin. Nat Rev Gastroenterol Hepatol. 2011;8(7),385–394. https://doi.org/10.1038/nrgastro.2011.97
7. Lin, S. et al. Preparation of novel anthraquinone-based aspirin derivatives with anti-cancer activity. Eur J Pharmacol. 2021;900:174020. https://doi.org/10.1016/j.ejphar.2021.174020
8. Rubner, G., Bensdorf, K., Wellner, A., Bergemann, S. & Gust, R. Synthesis, characterisation and biological evaluation of copper and silver complexes based on acetylsalicylic acid. Arch Pharm (Weinheim). 2011;344(10):684–688. https://doi.org/10.1002/ardp.201000382
9. Molinuevo, M. S., Etcheverry, S. B. &Cortizo, A. M. Macrophage activation by a vanadyl-aspirin complex is dependent on L-type calcium channel and the generation of nitric oxide. Toxicology. 2005;210(2-3):205–212. https://doi.org/10.1016/j.tox.2005.02.016
10. Salla, M. et al. Resveratrol and resveratrol-aspirin hybrid compounds as potent intestinal anti-inflammatory and anti-tumor drugs. Molecules. 2020;25(17):3849. https://doi.org/10.3390/molecules25173849
11. Turnbull, C. M. et al. Mechanism of action of novel NO-releasing furoxan derivatives of aspirin in human platelets. Br J Pharmacol. 2006;148(4): 517–526. https://doi.org/10.1038/sj.bjp.0706743
12. Mahdi, A. K. &Aljamali, N. M. Cell Biology and Cellular Processes Heterocyclic- Derivatives with Aspirin Drug (Synthesis , Characterization , Studying of Its Effect on Cancer Cells). International Journal of Cell Biology and Cellular Processes. 2020;6:1–20.
13. Yoosefian, M., Raissi, H., Davamdar, E., Esmaeili, A. A. &Azaroon, M. Synthesis and theoretical study of intramolecular hydrogen bond at two possible positions in pyrazolo[1,2-b]phthalazine. Chin J Chem. 2012;30:779–784. https://doi.org/10.1002/cjoc.201100036
14. Raissi, H., Yoosefian, M., Mollania, F. & Farzad, F. The effect of substitution on structure, intramolecular hydrogen bonding strength, electron density and resonance in 3-amino 2-iminomethyl acryl aldehyde. J Theor Comput Chem. 2012;11:925–939. https://doi.org/10.1142/S0219633612500629
15. Koll, A., Karpfen, A. &Wolschann, P. Structural and energetic consequences of the formation of intramolecular hydrogen bonds. J Mol Struct. 2006;790(1-3): 55–64. https://doi.org/10.1016/j.molstruc.2006.03.029
16. Kefah Mahdi, A. & Mahmood Aljamali, N. Heterocyclic-Derivatives with Aspirin Drug (Synthesis, Characterization, Studying of Its Effect on Cancer Cells). International Journal of Cell Biology and Cellular Processes. 2021;6(2):1-20.
17. Kim, S. et al. PubChem substance and compound databases. Nucleic Acids Res. 2016;44(1): D1202–D1213. https://doi.org/10.1093/nar/gkv951
18. Hratchian, H. P., Keith, T. A. & Millam, J. Gaussian 05 User's Reference. 2009.
19. Allouche, A. Software News and Updates Gabedit — A Graphical User Interface for Computational Chemistry Softwares. J Comput Chem. 2012;32(1): 174–182. https://doi.org/10.1002/jcc.21600
20. Frisch, M. J. et al. Gaussian 09, Revision B.01. Gaussian 09, Revision B.01, Gaussian, Inc., Wallingford CT 1–20. 2009.
21. London F. Théoriequantique des courants interatomiques dans les combinaisonsaromatiques. J de Physique et

le Radium. 1937;8:397409. https://doi.org/10.1051/jphysrad:01937008012048900

22. Geerlings P, De Proft F, Langenaeker W. Conceptual density functional theory. Chem Rev. 2003;103(5):1793-873. https://doi.org/10.1021/cr990029p
23. Becke AD. The effect of the exchange-only gradient gradient correction. J Chem Phys. 1992;96:2155-60. https://doi.org/10.1063/1.462066
24. Lu L, Hu H, Hou H, Wang B. An improved B3LYP method in the calculation of organic thermochemistry and reactivity. Comput Theor Chem. 2012;1015(1):64-71.
25. Tirado-Rives J, Jorgensen WL. Performance of B3LYP density functional methods for a large set of organic molecules. J Chem Theory Comput. 2008;4(2):297-306. https://doi.org/10.1021/ct700248k
26. Uzzaman M. Physicochemical, spectral, molecular docking and ADMET studies of Bisphenol analogues; A computational approach. Inform Med Unlocked. 2021;25:100706. https://doi.org/10.1016/j.imu.2021.100706
27. Petersilka M, Gossmann UJ, Gross EKU. Excitation energies from time-dependent density-functional theory. Phys Rev Lett. 1996;76(1):1212-5.
28. Temml V, Kutil Z. Structure-based molecular modeling in SAR analysis and lead optimization. Comput Struct Biotechnol J. 2021;19:1431-44.
29. Feng Y. Bisphenol AF may cause testosterone reduction by directly affecting testis function in adult male rats. Toxicol Lett. 2012;211(2):201-9.
30. Bryan PN. Protein engineering. Biotechnol Adv. 1987;5. https://doi.org/10.1016/0734-9750(87)90319-3
31. Wang J, Wolf RM, Caldwell JW, Kollman PA, Case DA. Development and testing of a general Amber force field. J Comput Chem. 2004;25(9):1157-74.
32. Harrach MF, Drossel B. Structure and dynamics of TIP3P, TIP4P, and TIP5P water near smooth and atomistic walls of different hydroaffinity. J Chem Phys. 2014;140(17):174501. https://doi.org/10.1063/1.4872239
33. Krieger E, Nielsen JE, Spronk CAEM, Vriend G. Fast empirical pKa prediction by Ewald summation. J Mol Graph Model. 2006;25(4):481-6.
34. Cheng F. AdmetSAR: A comprehensive source and free tool for assessment of chemical ADMET properties. J Chem Inf Model. 2012;52(11):3099-105.
35. Richel A, Laurent P, Wathelet B, Wathelet JP, Paquot M. Microwaveassisted conversion of carbohydrates. State of the art and outlook. Comptes Rendus Chimie. 2011;14(2-3):224-34. https://doi.org/10.1016/S1631-0748(11)00211-6
36. De Oliveira DB, Gaudio AC. BuildQSAR: A new computer program for QSAR analysis. Quantitative Structure-Activity Relationships. 2001;19(1):599-601.
37. Roux MV, Temprado M, Chickos JS, Nagano Y. Critically evaluated thermochemical properties of polycyclic aromatic hydrocarbons. J Phys Chem Ref Data. 2008;37(4):1855-996.
38. Uzzaman M, Uddin MN. Optimization of structures, biochemical properties of ketorolac and its degradation products based on computational studies. DARU. J Pharm Sci. 2019;27(1):71-82. https://doi.org/10.1007/s40199-019-00243-w
39. Liu Y. Is the free energy change of adsorption correctly calculated? J Chem Eng Data. 2009;54:1981-5. https://doi.org/10.1021/je800661q
40. Chen D. Bisphenol Analogues Other Than BPA: Environmental Occurrence, Human Exposure, and Toxicity - A Review. Env Sci Technol. 2016;50(11):5438-53. https://doi.org/10.1021/acs.est.5b05387
41. Hongyan L. Study on transformation and degradation of bisphenol A by Trametes versicolor laccase and simulation of molecular docking. Chemosphere. 2019;224(1):743-50. https://doi.org/10.1016/j.chemosphere.2019.02.143
42. Rosenfeldt EJ, Linden KG. Degradation of endocrine disrupting chemicals bisphenol A, ethinyl estradiol, and estradiol during UV photolysis and advanced oxidation processes. Environ Sci Technol. 2004;38(20):5476-83.
43. Lienx EJ, Guo ZR, Li RL, Su CT. Use of Dipole Moment as a Parameter in Drug-Receptor Interaction and Quantitative StructureActivity Relationship Stud. J Pharm Sci. 1982;71(6):641-55. https://doi.org/10.1002/jps.2600710611
44. Aihara JI. Reduced HOMO-LUMO Gap as an Index of Kinetic Stability for Polycyclic Aromatic Hydrocarbons. J Physical Chem. 1999;103(37):7487-95.
45. Saravanan S, Balachandran V. Quantum chemical studies, natural bond orbital analysis and thermodynamic function of 2,5-dichlorophenylisocyanate. Spectrochim Acta A Mol Biomol Spectrosc. 2014;120:351-64. https://doi.org/10.1016/j.desal.2014.07.038
46. Azam F. NSAIDs as potential treatment option for preventing amyloid β toxicity in Alzheimer's disease: an investigation by docking, molecular dynamics, and DFT studies. J Biomol Struct Dyn. 2018;36(8):2099-117.
47. Ayers PW, Parr RG, Pearson RG. Elucidating the hard/soft acid/base principle: A perspective based on half-reactions. J Chem Phys. 2006;124(19):194107.
48. Uzzaman M, Hoque MJ. Physiochemical, molecular docking, and pharmacokinetic studies of Naproxen and its modified derivatives based on DFT. Int J Sci Res Manag. 2018;6(9):2018.
49. Scrocco E, Tomasi PJ. The Electrostatic Molecular Potential as a Tool for the Interpretation of Molecular Properties. 2018.
50. Matin MM. Synthesis, spectroscopic characterization, molecular docking, and ADMET studies of mannopyranoside esters as antimicrobial agents. J Mol Struct. 2020;1222.
51. Ramalingam S, Karabacak M, Periandy S, Puviarasan N, Tanuja D. Spectroscopic (infrared, Raman, UV and NMR) analysis, Gaussian hybrid computational investigation (MEP maps/HOMO and LUMO) on cyclohexanone oxime. Spectrochim Acta A Mol BiomolSpectrosc. 2012;96:207-20.
52. Murray JS, Politzer P. The electrostatic potential: An overview. Wiley Interdiscip Rev Comput Mol Sci. 2011;1:153-63.
53. Merrick JP, Moran D, Radom L. An evaluation of harmonic vibrational frequency scale factors. J Phys Chem. 2007;111(45):11683-700. https://doi.org/10.1021/jp073974n
54. Halim MA, Shaw DM, Poirier RA. Medium effect on the equilibrium geometries, vibrational frequencies and solvation energies of sulfanilamide. J Molecular Structure: THEOCHEM. 2010;960(1-3):63-72.

55. Benecyo JE. Scholarly Commons @ Ouachita Scholarly Commons @ Ouachita Simultaneous Determination of BPA and BPS Using UV/Vis Simultaneous Determination of BPA and BPS Using UV/Vis Spectrophotometry and HPLC Spectrophotometry and HPLC. https://scholarlycommons.obu.edu/honors_theses/233.
56. Uzzaman M. Physicochemical, spectral, molecular docking and ADMET studies of Bisphenol analogues; A computational approach. Inform Med Unlocked. 2021;25. https://doi.org/10.1016/j.imu.2021.100667
57. Lengauer T, Rareyt M. Computational methods for biomolecular docking. Current Opinion in Structural Biol. 1996;6(3):402-6. https://doi.org/10.1016/S0959-440X(96)80061-3
58. Varma AK. Optimized hydrophobic interactions and hydrogen bonding at the target-ligand interface leads the pathways of Drug Designing. PLoS One. 2010;5(8):e12029. https://doi.org/10.1371/journal.pone.0012029
59. Matin MM. Synthesis, characterization, ADMET, PASS predication, and antimicrobial study of 6-O-lauroyl mannopyranosides. J Mol Struct. 2019;1195(5):189-97.
60. Meyer EA. Interactions with Arenes Interactions with Aromatic Rings in Chemical and Biological Recognition Angewandte Chemie Keywords: arenes • hydrogen bonds • molecular recognition noncovalent interactions • receptors Dedicated to Professor Dieter Seebach. Angew Chem Int 2003;42.
61. Uzzaman M, Hasan MK, Mahmud S, Fatema K, Matin MM. Structure-based design of new diclofenac: Physicochemical, spectral, molecular docking, dynamics simulation and ADMET studies. Inform Med Unlocked. 2021;25(5):100677. https://doi.org/10.1016/j.imu.2021.100677
62. Shen J, Cheng F, Xu Y, Li W, Tang Y. Estimation of ADME properties with substructure pattern recognition. J Chem Info Model. 2010;50(6):1034-41. https://doi.org/10.1021/ci100104j
63. Szczeklik A, Gryglewski RJ, Czaizniawska-Mysik G. Relationship of Inhibition of Prostaglandin Biosynthesis by Analgesics to Asthma Attacks in Aspirin-sensitive Patients. Br Med J. 1975;1(5949):67-9. https://doi.org/10.1136/bmj.1.5949.67
64. Hubatsch I, Ragnarsson EGE, Artursson P. Determination of drug permeability and prediction of drug absorption in Caco-2 monolayers. Nat Protoc. 2007;2(9):2111-9. https://doi.org/10.1038/nprot.2007.303
65. The HP. In silico prediction of caco-2 cell permeability by a classification QSAR approach. Mol Inform. 2011;30(4):376-85. https://doi.org/10.1002/minf.201000118
66. Bickerton GR, Paolini GV, Besnard J, Muresan S, Hopkins AL. Quantifying the chemical beauty of drugs. Nat Chem. 2012;4(2):90-8. https://doi.org/10.1038/nchem.1243
67. Wang RB, Kuo CL, Lien LL, Lien EJ. Structure-activity relationship: Analyses of p-glycoprotein substrates and inhibitors. J Clin Pharm Ther. 2003;28(3):203-28. https://doi.org/10.1016/S0925-5214(03)00034-6
68. Amin ML. P-glycoprotein inhibition for optimal drug delivery. Drug Target Insights. 2013;7:27-34. https://doi.org/10.1016/j.displa.2012.11.005
69. Finch A, Pillans P. P-glycoprotein and its role in drug-drug interactions. Aust Prescr. 2014;37:137-9. https://doi.org/10.18773/austprescr.2014.050
70. Didziapetris R, Japertas P, Avdeef A, Petrauskas A. Classification analysis of P-glycoprotein substrate specificity. J Drug Target. 2003;11(7):391-406.
71. Carbon-Mangels M, Hutter MC. Selecting relevant descriptors for classification by Bayesian estimates: A comparison with decision trees and support vector machines approaches for disparate data sets. Mol Inform. 2011;30(10):885-95. https://doi.org/10.1002/minf.201100069
72. Lamothe SM, Guo J, Li W, Yang T, Zhang S. The Human Ethera-go-go-related Gene (hERG) potassium channel represents an unusual target for protease-mediated damage. J Biol Chem. 2016;291(39):20387-401.
73. Filimonov DA. Prediction of the biological activity spectra of organic compounds using the pass online web resource. Chem HeterocyclCompd (NY). 2014;50(3):444-57.
74. Lagunin A, Stepanchikova A, Filimonov D, Poroikov V. PASS: Prediction of activity spectra for biologically active substances. Bioinformatics. 2000;16(8):747-8. https://doi.org/10.1093/bioinformatics/16.8.747
75. Lagunin A, Zakharov A, Filimonov D, Poroikov V. QSAR modeling of rat acute toxicity on the basis of PASS prediction. Mol Inform. 2011;30(2-3):241-50.
76. Zhu H. Quantitative structure-activity relationship modeling of rat acute toxicity by oral exposure. Chem Res Toxicol. 2009;22(12):1913-21. https://doi.org/10.1021/tx900189p

Cite this article: Kabir E, Noyon MROK, Hossain MA, Acharjee P. DFT and Pharmacokinetic Study of Some Heterocyclic Aspirin Derivatives as the Cyclooxygenase Inhibitors: An *In-Silico* Approach. Pharmacogn J. 2022;14(6)Suppl: 1005-1021.